X-ray diffraction and Mössbauer studies of NiFe₂O₄ nanoparticles obtained by co-precipitation method

E. Agouriane[1,*], A. Essoumhi[1,2], A. Razouk[1], M. Sahlaoui[1], M. Sajieddine[1,*]

[1]*Laboratoire de Physique des Matériaux, FST, Université Sultan Moulay Slimane, Béni-Mellal, Maroc*

[2]*Laboratoire Interdisciplinaire de Recherche en Sciences et Techniques, F.P., Université Sultan Moulay Slimane, Béni-Mellal, Maroc*

Abstract

Spinel nickel ferrite NiFe₂O₄ nanoparticles were synthesized by co-precipitation method and annealed at different temperatures 600, 800 and 1000°C. The structural and magnetic properties of the nanoparticles are characterized by thermogravimetric analysis, X-ray diffraction and Mössbauer spectrometry. The lattice parameter, the crystallite size and the cation distribution have been determined by Rietveld method for the sample annealed at 1000°C. The hyperfine parameters are determined by Mössbauer spectrometry at room temperature. The hyperfine field increases with crystallite size.

Keywords: Spinel structure, nickel ferrite, cation distribution, Rietveld refinement, magnetic properties.

1.Introduction

For the last few decades, the ferrites nanoparticles have been extensively studied due to their significant different applications such as optical, electrical and magnetic properties which are different from their bulk structure [1-9]. In particular, nickel ferrite has an interesting set of properties making it in a wide range of applications such as in the radio frequency, magnetic resonance imaging contrast agents for biotechnology, and magnetic nano-fluid for hyperthermia cancer treatments[10-13]. Several methods for the synthesis of nickel-based ferrite nanoparticles are used and which include co-precipitation [14], mechanical alloying [15], sol-gel method [16], combustion [17], ... The performance of the NiFe₂O₄ are highly dependent on the structural and magnetic properties which are also influenced by particle size and shape might be controlled in the fabrication processes. For example, Ojha et al [21] show that the NiFe₂O₄ nanoparticles prepared by sol-gel method exhibit ferromagnetic behavior at room temperature, whereas nanoparticles prepared by hydrothermal process show a super-paramagnetic behavior at the same temperature. According to their crystallographic structure, spinel ferrite has a tetrahedral A-site and octahedral B-site in MFe₂O₄ [11,19]. The physical properties of ferrites are strongly affected by the cation distribution among A and B-sites which can be represented generally by the formula:

$$(M_{1-x}^{2+}Fe_x^{3+})_A\left[M_x^{2+}Fe_{2-x}^{3+}\right]_B O_4^{2-}.$$
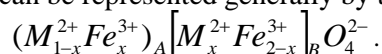
The aim of the present work is to prepare NiFe₂O₄ nanoparticles by co-precipitation and to study the effect of the annealing temperature on the obtained phases, and then the structural parameters and magnetic properties are investigated. The thermal decomposition behavior was examined by means of thermogravimetry TG and differential thermal analysis DTA. The structural characterization of the samples was characterized by X-Ray diffraction and the magnetic properties were explored by transmission[57]Fe Mössbauer spectrometry at room temperature.

2. Experimental

Nickel ferrite nanoparticles were prepared by co-precipitation method. Nickel(II) nitrate hexahydrate $Ni(NO_3)_2.6H_2O$ and iron(III) chloride hexahydrate $FeCl_3 \cdot 6H_2O$ analytical grade were used in stoichiometric proportion as starting materials.

The mixture was dissolved in 100 ml of distilled water and stirred continuously for 30 min under constant heating at 40°C to initiate a self-propagating exothermic reaction. The precipitation was performed by adding sodium hydroxide NaOH (1M) until pH equal to 12. The resulting product was washed several time by distilled water and dried at 80°C for 24h. Finally, the product was annealed in air at different temperatures 600, 800 and 1000°C for 2h.

In order to monitor the mass change of the samples during heating, TG and DTA experiments were conducted under synthetic air with the heating rate of 10°C/min, on a LabSys EVO Setaram 1600. The phase formation was examined by X-ray diffraction (XRD) spectra with Cu-K$_\alpha$ radiation (λ=1.5406Å) using a Bruker D-8 Advance X-ray diffractometer, at 40kV×40mA. The X-ray diffraction spectra were recorded at room temperature in 2θ angular range between 15 and 70° with a step size of 0.02°. The [57]Fe Mössbauer spectra were recorded at room temperature using a constant acceleration spectrometer with triangular velocity shape, and linear arrangement of the [57]Co source (25 mCi), absorber and detector. The spectrometer velocity was calibrated with a high purity α-Fe foil. The estimated isomer shifts (IS) are given relative to this standard. All spectra were measured at room temperature in transmission configuration of the Mössbauer spectrometer (Wissel).

3. Result and discussion

The TG-DTA results shown in Fig. 1 help in the selection of the calcination temperature. The first stage is reached at 30–150°C, which is attributed to the loss of water physisorbed. The second stage corresponding to the total loss of about 22% between 150 and 450°C is due to the departure of nitrate residue. After 450°C no significant weight loss was observed.
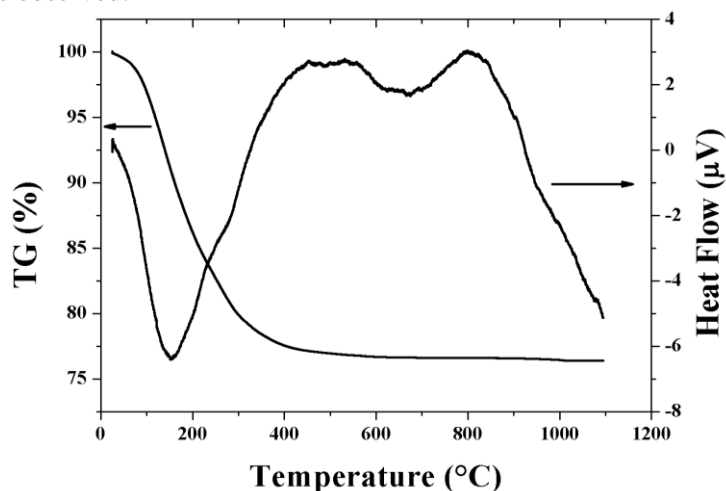

Figure 1: TG-DTA plot for the un-annealed sample

The XRD patterns of Nickel ferrite synthesized by coprecipitation and annealed at different temperatures are shown in Fig. 2. The patterns show the formation of single phase spinel structure of $NiFe_2O_4$ with space group symmetry $Fd\bar{3}m$ and without any trace of impurity peaks. The lattices parameters 'a' is calculated by using the formula $a = d\sqrt{h^2 + k^2 + l^2}$ where d is the inter-reticular distance and hkl are the Miller indices of the plan. The average crystallite size D of the nano-particles in the samples were calculated from the broadening of 100% intense peak (311) of each sample by using the Debye–Scherrer equation [20]. Eva software was used for data processing and evaluation of the degree of crystallinity (C). All these parameters are summarized in Table 1.
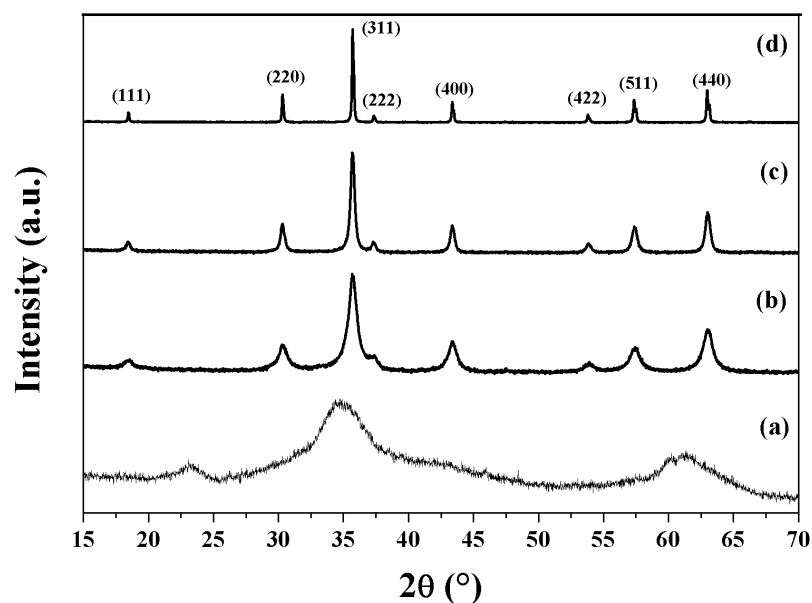
Figure 2: X-ray diffraction patterns of the un-annealed (a) and the annealed samples 600°C (b), 800°C (c) and 1000°C (d).

Table 1: Structural parameters *a*, *D* and *C* for the annealed samples

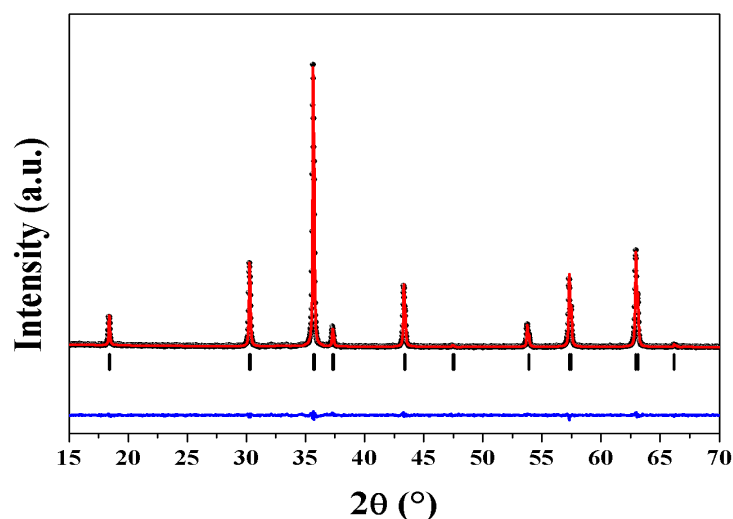| *T* (°C)	*a* (Å)	*D* (nm)	*C* (%)
600	8.345	12	75.5
800	8.343	25	84.6
1000	8.334	82	90.5

Figure 3: Rietveld refinement pattern for the sample annealed at 1000°C. The experimental data are in black circles and the Rietveld refinement is in red line. The blue line is the difference between the experimental and calculated intensities.

$NiFe_2O_4$ has an inverse spinel structure in which, in its ideal state, all Ni^{2+} ions are in B-sites and Fe^{3+} ions are equally distributed between A and B-sites [11, 13]. Based on the mention above, the Rietveld refinement of X-ray diffraction patterns for sample annealed at 1000°C is carried out (Fig. 3). The Solid line is the best fit to the data,

the tic marks show the positions for the allowed reflections, and the lower curve represents the difference between the observed and the calculated profiles.

The Rietveld structure refinement was carried out using FULLPROF-suite software from X-ray powder diffraction data. The structural model and initial structural parameters were taken as follows: space group $Fd\overline{3}m$, nickel and iron atoms were in 8a and 16d special position and oxygen atom in 32e special positions. The refinement is done using the pseudo-Voigt profile function.

The quality of the agreement between observed and calculated profiles is checked by using the goodness of fit χ^2 and two reliability factors R_p and R_{wp} [21-22]. χ^2 must tend to 1, R_p and R_{wp} must be less than 10% for good quality of refinement [21,23]. In our case, $\chi^2 =1.21$, R_p=2.86 and R_{wp} =3.70.

Table 2 gives the structural parameters and Rietveld agreement factors for the sample annealed at 1000°C : the degree of inversion 'x', the lattice parameter 'a', the oxygen position parameter 'u' and the mean particles size 'D'.

Table 2: Structural parameter obtained from Rietveld refinement.

Parameters	Value
Space group	$Fd\overline{3}m$ (#227)
Degree of inversion x	0.95011
Oxygen parameter u	0.255
Lattice parameter a (Å)	8.346
D (nm)	81.7
χ^2	1.21
R_p (%)	2.86
R_{wp} (%)	3.70

As seen in table 2, the calculated crystallite size and the lattice parameter of the nanoparticles are in good agreement with those, given in table 1.

The cation distribution is represented by the inversion parameter x, occupancies of Fe^{3+} ions at the A-site is equal to 0.95. This value is very close to 1 corresponding to an inverse spinel structure which is in good agreement with that observed in the bulk structure [24,25].

Mössbauer spectra of the samples, acquired at room temperature without external magnetic field are presented in Fig. 4.
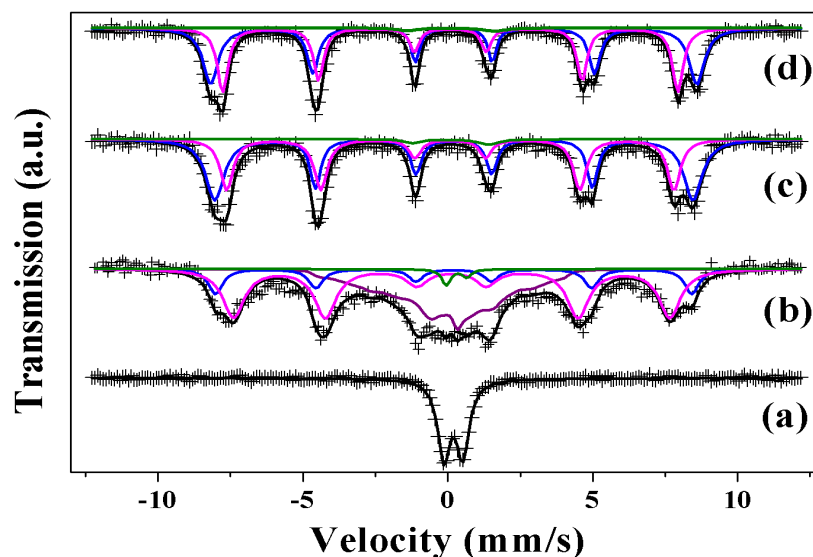

Figure 4: Mössbauer spectra recorded at room temperature for the un-annealed (a) and annealed samples at 600°C (b), 800°C (c) and 1000°C (d).

For the un-annealed sample, the Mössbauer spectrum consists of a doublet with a quadrupole splitting ΔE_Q of 0.65 mm/s, and an isomer shift *IS* of 0.34 mm/s. This reflects the fact that the iron atoms in the sample is in a purely paramagnetic phase.The shapes of the samples annealed at 800 and 1000°C are characteristic of iron atoms in magnetic state and are essentially composed of two more or less strongly overlapping sextets related to the presence of iron in tetrahedral sites (A-sites) and octahedral sites (B-sites). To have the best fit of the spectra, we have superimposed three components: two components in the form of sextet with different hyperfine fields reflecting that iron is found in two different environments, and the third one is a doublet with low weight (~2% of the total area of the spectra) representing iron atoms in paramagnetic state.

The spectrum relating to the sample annealed at 600°C has a shape intermediate between those of the un-annealed sample and annealed samples at 800 and 1000°C. The adjustment of the spectrum requires a fourth component : the three components described above and a broad magnetic component indicating the presence of distribution of magnetic hyperfine fields. We have been analysed in terms of distribution of hyperfine field P(H$_{hyp}$), this component represents 37% of the total area of the spectrum.

Table 3: Hyperfine parameters obtained from fitting Mössbauer spectra.

T (°C)	Component	H_{hyp} (kOe)	IS (mm/s)	QS (mm/s)	A (%)
Un-annealed	Doublet	-	0.343	0.65	100
600	Sextet	460.4	0.287	-	45.65
	Sextet	510.4	0.358	-	15.26
	Distribution	133	0.364	-	37.07
	Doublet	-	0.456	0.73	2.02
800	Sextet	479.3	0.238	-	42.23
	Sextet	512.4	0.362	-	55.37
	Doublet	-	0.260	2.6	2.40
1000	Sextet	487.9	0.244	-	45.95
	Sextet	521.1	0.362	-	52.18
	Doublet	-	0.263	3	1.87

The inversion parameters calculated from the relative area (*A*) covered by the sextets corresponding to the A and B sites for the sample annealed at 1000°C is estimated to 0.97. This value is in good agreement with that found by Rietveld refinement 0.95. In Fig. 5, we have presented the evolution of the average hyperfine field <*H*$_{hyp}$> versus the crystallite size.We can observe that <*H*$_{hyp}$> increases with crystallite size since the field is proportional to the volume of the crystallite [26]. We note that the average hyperfine field increases significantly for smaller particle sizes (from 12 to 25 nm).
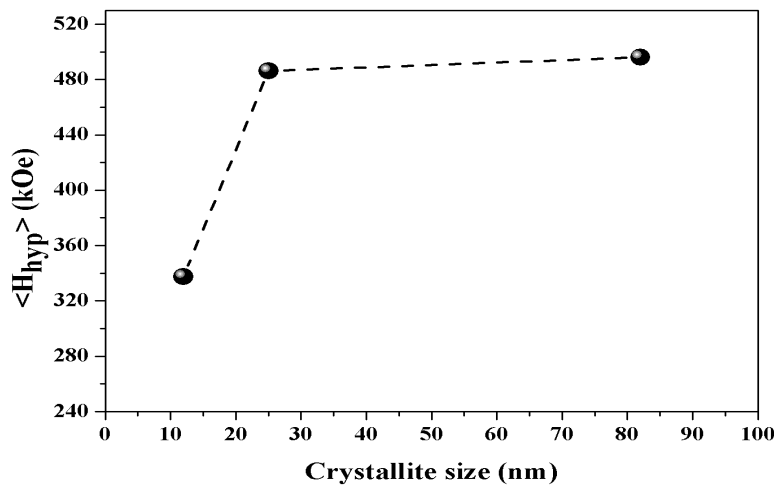

Figure 5: Effect of crystallite size on the hyperfine filed

Conclusion

In this work, $NiFe_2O_4$ nanoparticles were synthesized by co-precipitation and annealed at 600, 800 and 1000°C. The XRD analysis indicated the formation of single phase spinel structure. Rietveld refinement of the X-ray diffraction data revealed that the sample possess cubic symmetry corresponding to the space group $Fd\bar{3}m$. For the sample annealed at 1000°C, cations distribution show that $NiFe_2O_4$ have an inverse spinel structure and the inversion parameter agrees with the value deduced from Mössbauer spectrometry measurements at room temperature.

References

1. Rais A., Taibi K., Addou A., Zanoun A., Al-Douri Y., *Ceram. Int.* 40 (2014) 14413.
2. Zaki H.M., Al-Heniti S.H., Elmosalami T.A., *J. Alloys Compd.* 633 (2015) 104.
3. Patil D.R., Chougule B.K., *Mat. Chem. and Phy.* 117 (2009) 35.
4. Tan X., Li G., Zhao Y., Hu C., *Mater. Res. Bull.* 44 (2009) 2160.
5. Gabal M.A., Al-Angari Y.M., *Mat. Chem. Phys.*115 (2009) 578.
6. Duquenne P., Deltour A., Lacoste G.,*Inter. J. Heat and Mass Trans.*36 (1993) 2473.
7. Suk Fun Chin, Suh Cem Pang, Ching Hong Tan, *J. Mater. Environ. Sci.* 2 (3) (2011) 299.
8. El Jabbar Y., El Ouatib R., Er-Rakho L., Durand B., *J. Mater. Environ. Sci.* 6 (12) (2015) 3452.
9. Agouriane E., Rabi B., Essoumhi A., Razouk A., Sahlaoui M., Costa B.F.O., Sajieddine M., J. Mater. Environ. Sci. 7 (11) (2016) 4116.
10. Benrabaa R., Boukhlouf H., Löfberg A., Rubbens A.,Vannier R.N., Bordes-Richard E., Barama A., *J. Nat. Gas Chem.* 21 (2012) 595.
11. Joshi S., Kumar M., Chhoker S., Srivastava G., Jewariya M., Singh V.N., *J. Molecular Structure* 1076 (2014) 55.
12. Streckova M., Hadraba H., Bures R., Faberova M., Roupcova P., Kubena I., Medvecky L.,Girman V., Kollar P., Fuzer J., Cizmar E., *Surf. Coat. Techn.* 270 (2015) 66.
13. Dong-yun Lia, Yu-kun Sun, Peng-Zhao Gao, Xiao-Liang Zhang, Hong-Liang Ge, *Ceram. Int.* 40 (2014) 16529.
14. Maaz K., Mumtaz A., Hasanain S.K., Bertino M.F., *J. Magn. Magn. Mater.*322 (2010) 2199.
15. Shi Y, Ding J., Liu X., Wang J., *J. Magn. Magn.Mater.* 205 (1999) 249.
16. Rakesh Malik, Annapoorni S., SubhalakshmiLamba, Raghavendra Reddy V., Ajay Gupta, Parmanand Sharma, Akihisa Inoue*, J. Magn. Magn.Mater.*322 (2010) 3742.
17. Elshahawy A.M., Mahmoud M.H., Makhlouf S.A., Hamdesh H.H., *Ceram. Int.* 41 (2015) 11264.
18. Manish Srivastava, Chaubey S., AnimeshOjha K., *Mat. Chem. and Phy*. 118 (2009) 174.
19. Marinca T.F., Chicinas I., Isnard O., *Ceram. Int.* 38 (2012) 1951.
20. Cullity B.D., Elements of X-Ray Diffraction, *Addison-Wesley Publishing Company, Inc*. USA, (1978).
21. Gomes J.A., Sousa M.H., Tourinho F.A., Mestnik-Filho J., Itri R., Depeyrot J., *J. Magn. Magn. Mater.*289 (2005) 184.
22. Ke Sun, Zhiyong Pu, Yan Yang, Ling long Chen, Zhong Yu, Chuanjian Wu, Xiaona Jiang, Zhongwen Lan, *J. Alloys Compd*. 681 (2016) 139.
23. Ko D., Poeppelmeier K.R., Kammler D.R., Gonzalez G.B., Mason T.O., Williamson D.L., Young D.L., Coutts T.J., *J. Solid State Chem*. 163 (2002) 259.
24. Roisnel T., Rodriquez-Carvajal J., *Mat. Sci. Forum* 378-381 (2001) 118.
25. Moradmard H., Farjami Shayesteh S., Tohidi P., Abbas Z., Khaleghi M., *J. Alloys Compd*. 650 (2015) 116.
26. Muhammad Javed Iqbal, Yaqub Nadia, Bogdan Sepiol, Bushra Ismail, *Mat. Res. Bull.* 46 (2011) 1837.